NASA TECHNICAL MEMORANDUM

NASA TM-73826

NASA TM-73826

THE EFFECTS OF ECCENTRICITIES ON THE FRACTURE OF OFF-AXIS FIBER COMPOSITES

by C. C. Chamis and J. H. Sinclair
Lewis Research Center
Cleveland, Ohio 44135

TECHNICAL PAPER to be presented at the Thirty-third Annual Conference of the Society of the Plastics Industry Reinforced Plastics/Composites Institute
Washington, D.C., February 7-10, 1978

-- ((ENTER NEXT COMMAND))

-- 1 OF 1
-- ***DTIC DOES NOT HAVE THIS ITEM***
-- 1 - AD NUMBER: D425720
-- 5 - CORPORATE AUTHOR: NATIONAL AERONAUTICS AND SPACE ADMINISTRATION
-- CLEVELAND OHIO LEWIS RESEARCH CENTER
-- 6 - UNCLASSIFIED TITLE: THE EFFECTS OF ECCENTRICITIES ON THE
-- FRACTURE OF OFF-AXIS FIBER COMPOSITES,
--10 - PERSONAL AUTHORS: CHAMIS ,C. C. ;SINCLAIR,J. H. ;
--11 - REPORT DATE: FEB 07, 1978
--12 - PAGINATION: 17P
--14 - REPORT NUMBER: NASA TM-73826, E-9269-1
--20 - REPORT CLASSIFICATION: UNCLASSIFIED
--21 - SUPPLEMENTARY NOTE: PRESENTED AT 33RD ANNUAL CONFERENCE OF THE
-- PLASTICS INDUSTRY REINFORCED PLASTICS/COMPOSITES INSTITUTE, 7-10
-- FEB 78, WASHINGTON, D.C.
--22 - LIMITATIONS (ALPHA): APPROVED FOR PUBLIC RELEASE; DISTRIBUTION
-- UNLIMITED. AVAILABILITY: NATIONAL TECHNICAL INFORMATION SERVICE,
-- SPRINGFIELD, VA. 22161. N76-17152.
--33 - LIMITATION CODES: 1

-- END Y FOR NEXT ACCESSION END

THE EFFECTS OF ECCENTRICITIES ON THE FRACTURE OF OFF-AXIS FIBER COMPOSITES

by C. C. Chamis* and J. H. Sinclair*

National Aeronautics and Space Administration
Lewis Research Center
Cleveland, Ohio 44135

E-9269-1

ABSTRACT

Finite element analyses were performed to investigate theoretically the effects of in-plane and out-of-plane eccentricities, bending or twisting, and thickness nonuniformity on the axial stress and strain variations across the width of off-axis specimens. The results are compared with measured data and are also used to assess the effects of these eccentricities on the fracture stress of off-axis fiber composites. Guidelines for detecting and minimizing the presence of eccentricities are described.

INTRODUCTION

Off-axis tensile data for unidirectional composites are of considerable interest to the fiber composite community for several important reasons. Some of these are: (1) determination of the variation of elastic properties and fracture stress (strain) as a function of load angle (angle between fiber and load directions), (2) verification of composite macromechanics theories for elastic properties and for combined-stress fracture, and (3) generation of fundamental information for assessing angleplied laminate mechanical behavior.

---

*Aerospace and Materials Engineer, respectively, Composites and Structures Branch, NASA.

An extensive investigation was conducted to study the mechanical behavior and fracture characteristics of off-axis fiber composites (refs. 1 and 2). Specimens of MODI/E (graphite reinforced epoxy) were proposed and tested with load angles varying from 0 to 90^{o} with the fiber direction. It was found in that investigation that in-plane and out-of-plane eccentricities affect the stress (strain) variation across the width of the specimen significantly. The effects of these eccentricities on the tensile strain (stress) variation and fracture of off-axis fiber composites are examined herein using finite element analyses. Also the effects of nonuniform specimen thickness on strain (stress) variations and fractures are examined using finite element analysis. The results obtained are compared with measured data and are used to: (1) assess the effects of eccentricities on off-axis composite tensile fracture and (2) establish guidelines for detecting and minimizing eccentricities during testing.

IN-PLANE BENDING EFFECTS

Off-axis tensile specimens will tend to undergo in-plane bending. This is caused by the coupling between normal and shear deformations: this coupling will tend to deform the specimen in shear. However, the grips prevent the specimen ends from shearing, thereby inducing in-plane bending. This in-plane bending induces axial stress and strain variations across the specimen width. These variations are determined theoretically herein using finite-element analysis.

The finite element used in the analysis is a second-order triangular plate finite element with six nodes and two displacement degrees

of freedom per node. A schematic of the finite-element representation is shown in figure 1. The dimensions used in the analysis were those of the actual test specimens. Those shown in the schematic are for the 10° off-axis test specimen. Note that the finite-element representation includes the tapered end-tab portions projecting beyond the grip ends. Note also that the finite-element representation consists of 288 elements, 657 nodes, and 1314 degrees of freedom.

Finite-element analysis results for the axial stress variation, near the end tab (node line 73 to 81, fig. 1) are summarized graphically in figure 2. These stress variations were determined using the fracture loads of the specimens and the elastic constants summarized in table I. As can be seen in figure 2, the most significant axial stress variation is for the 10° off-axis specimen with a maximum difference of 16.6×10^3 N/cm^2 (24 ksi) from edge-to-edge (46×10^3 to 30×10^3 N/cm^2 (67 to 43 ksi)). Additional discussion on this variation is given in reference 3. The next most significant axial stress variation is that for the 15° off-axis specimen with a maximum difference of 7.8×10^3 N/cm^2 (13 ksi) from edge-to-edge (26×10^3 to 17×10^3 N/cm^2 (38 to 25 ksi)). The axial stress variation for the remaining specimens is relatively mild and may be considered as insignificant. An interesting result shown in figure 2 is the stress reversal trend from 5° (increasing left to right) to 10° (decreasing).

The important observation from the preceding discussion is that off-axis tensile specimens show high axial stresses at the edges near the grips in the 5° to 15° load angle range and, consequently, fracture

should initiate in this region.

Corresponding results for the axial stress variation are shown in figure 3. Here, again, the significant axial strain variation across the specimen width is for the 10^{o} and 15^{o} off-axis specimens. These results illustrate the importance of placing strain gages as close to the edge as possible near the end-tab region.

Finite-element results for the axial stress variation at the specimen midlength (center) are shown in figure 4. Only the 10^{o} off-axis specimen shows a significant variation (about 9×10^{3} N/cm^{2} (13 ksi)) from edge-to-edge (39×10^{3} N/cm^{2} to 30×10^{3} N/cm^{2} (56 to 43 ksi)). Corresponding results for axial strain are shown in figure 5. As can be seen in this figure, only the 10^{o} and 15^{o} off-axis specimens show significant variations from edge-to-edge.

The important observation here is that in-plane bending produces significant axial stress variation at midlength only in the 10^{o} off-axis specimen. The significance of this observation is that the P/A (fracture load/cross-section-area) stress is a very good approximation to the actual axial stress at the center of the off-axis specimens. And, in addition, the fracture stress determined from P/A would probably be on the conservative side. It is important to keep in mind that these comments apply to specimens with the gage length-to-width ratios tested herein, which were 14 or greater.

Comparison of finite-element predicted axial strains with measured data near the specimen end tab at fracture load are shown in figure 6. Corresponding results at the specimen midlength are shown

in figure 7. As can be seen from these figures, the agreement is reasonably good for the three specimens near the end tab and the 60^{o} specimen at midlength. However, the agreement for the 10^{o} and 30^{o} specimens at midlength is relatively poor. The predicted results are about 10 to 20 percent higher than the measured data at the left edge and center and are less than 10 percent at the right edge.

Some factors that may have contributed to this poor agreement between predicted and measured fracture strains at midlength of the 10^{o} and 30^{o} off-axis specimens are:

(1) Inability to simulate mathematically exactly the physical boundary conditions

(2) Nonlinear material behavior near fracture

(3) Out-of-plane eccentricities - bending and/or twisting

(4) Variation in specimen thickness

Item (1) was extensively studied via sensitivity analysis in reference 3 and found to have an effect of less than 5 percent. Item (2) is not believed to have any significant contribution because the stress strain curves (figs. 6 and 8, from ref. 1, Part I) are linear to fracture. Items (3) and (4) were investigated herein and are described in the next section. Note that item (3) was also discussed in reference 4.

OUT-OF-PLANE BENDING AND TWISTING EFFECTS

The effects of out-of-plane bending and twisting on axial strain were evaluated for the 10^{o} and 30^{o} off-axis specimens using NASTRAN (NASA Structural Analysis Finite Element Computer program,

ref. 5). The NASTRAN model of the specimen is shown in figure 8. The NASTRAN model consisted of 657 nodes (1971 degrees of freedom) and 576 quadrilateral plate bending elements, which included the tapered portion of the reinforcing end tabs. Note that the finite-element representation includes two groups of elements. At each end the elements are 0.159 centimeter (0.0625 in.) long; these represent the tapered portion of the reinforcing tabs and the first quarter inch segment of the test section, which is the site of the top strain gages. The remaining elements of the representation are 0.318 centimeters (0.125 in.) long. All elements for this model are 0.159 centimeters (0.0625 in.) wide. The element size was made small enough to study the zones where the strain gages were located on the actual specimen. The material properties required for NASTRAN were generated from the elastic constants in table I. The load for both the out-of-plane bending and twisting moments was 11.3 newton-meters (100 in.-lb). The value of 11.3 newton-meters (100 in.-lb) was selected mainly for convenience. It corresponds roughly to an eccentricity of a laminate thickness. The effects of smaller eccentricities are readily obtained by direct proportion since a linear stress analysis was performed.

NASTRAN undeformed and deformed plots due to out-of-plane bending moments are shown in figure 9 for the 10° off-axis specimen and in figure 10 for the 30° off-axis specimen. As can be seen in these plots the deformation for both bending and twisting are considerable.

The axial strain variation due to bending moments across the

specimen width predicted using NASTRAN is shown in figure 11 (solid lines for the 10° and interrupted lines for the 30° off-axis specimens). Corresponding results for axial strain variation at midlength are shown in figure 12. The curves in these figures show that the axial strain variation can be significant near the grips for both bending and twisting and at midlength for bending. This would tend to explain the differences between predicted and measured data shown in figures 6 and 7 and discussed previously.

Thus we see that out-of-plane eccentricities can contribute significantly to the axial strains. Therefore, care should be taken to keep them to an absolute minimum during testing of off-axis specimens.

THICKNESS VARIATION EFFECTS

The effects of specimen thickness variation on the axial strain were investigated using NASTRAN and actual measured thickness variations of the specimen (0.15 to 0.14 cm (0.059 to 0.055 in.)). The finite-element model used is shown in figure 8 and has already been described. The results obtained for the 5° off-axis specimen are compared with those for uniform thickness in figure 13. As can be observed from the curves in this figure the thickness variation effects are negligible.

GUIDELINES FOR DETECTING AND MINIMIZING ECCENTRICITIES

The following guidelines may be helpful in instrumenting specimens to detect the presence of out-of-plane eccentricities during testing:

(1) For out-of-plane bending, place strain gages back-to-back at the specimen edge (fig. 14).

(2) For out-of-plane twisting, place strain gages at both edges on the same surface of the specimen near the end tab (fig. 14).

(3) If, during testing, the differences in the readings from the pair of strain gages in (1) or (2) or both become excessively high (say, more than 15 percent), then stop the test and realine the specimen to minimize the out-of-plane eccentricities. The strains already recorded can be used to guide the direction of the realinement.

SUMMARY OF RESULTS AND CONCLUSIONS

The major results and conclusions of this investigation are:

1. The second-order triangular finite-element predicted results showed that in-plane bending has considerable influence on the axial strain variation across the width of the specimen. This influence is most significant in the 5° to 30° load-angle range. The predicted fracture strain variation was off by about 20 percent from the measured data.

2. NASTRAN predicted results showed that thickness variations in the specimen (0.14 to 0.15 cm (0.055 to 0.059 in.)) have negligible effect on the axial strain variation across the specimen width.

3. NASTRAN predicted results showed that out-of-plane bending and twisting eccentricities have significant effects on the axial strain variation across the width for specimens in the 10° to 30° load-angle range.

4. Care should be taken to minimize eccentricities that will induce out-of-plane bending and twisting since these eccentricities

have significant effect on the axial strain.

5. Fracture stress of off-axis tensile specimens determined by load to area ratio should be on the conservative side.

REFERENCES

1. J. H. Sinclair and C. C. Chamis, Mechanical Behavior and Fracture Characteristics of Off-Axis Fiber Composites. I - Experimental Investigation. NASA TP-1081, 1977.

2. C. C. Chamis and J. H. Sinclair, Mechanical Behavior and Fracture Characteristics of Off-Axis Fiber Composites. II - Theory and Comparisons. NASA TP-1082, 1977.

3. C. C. Chamis and J. H. Sinclair, 10^{o} Off-Axis Tensile Test for Intralaminar Shear Characterization of Fiber Composites. NASA TN D-8215, 1976.

4. C. C. Chamis, J. H. Sinclair, and T. L. Sullivan, NASTRAN as an Analytical Research Tool for Composite Mechanics and Composite Structures. NASA TM X-3428, 1976, pp. 381-417.

5. C. W. McCormick, NASTRAN User's Manual (Level 15). NASA SP-222 (01), 1972.

TABLE I. - PREDICTED COMPOSITE ELASTIC CONSTANTS - STRUCTURAL AXES FOR MOD I/E

[Used in finite-element analyses.]

Specimen	Load angle, deg	Composite elastic constants								
		Moduli						Poisson's ratio, ν_{cxy}	Coupling coefficients	
		E_{cxx}		E_{cyy}		E_{cxy}				
		N/cm^2	psi	N/cm^2	psi	N/cm^2	psi		ν_{cxs}	ν_{cys}
A-0	0	21.0×10^6	30.4×10^6	0.73×10^6	1.06×10^6	0.515×10^6	0.747×10^6	0.260	0	0
A-5	5	16.3	23.6	.73	1.06	.519	.753	.263	2.56	.053
A-10	10	9.79	14.2	.74	1.08	.531	.770	.265	3.00	.109
A-15	15	5.97	8.66	.77	1.11	.550	.798	.261	2.62	.170
A-30	30	2.12	3.07	.88	1.28	.638	.926	.225	1.44	.410
A-45	45	1.20	1.74	1.20	1.74	.696	1.01	.165	.793	.793
A-60	60	.88	1.28	2.12	3.07	.638	.926	.094	.410	1.44
A-75	75	.77	1.11	5.97	8.66	.550	.798	.033	.170	2.62
A-90	90	.73	1.06	21.0	30.4	.515	.747	.009	0	0

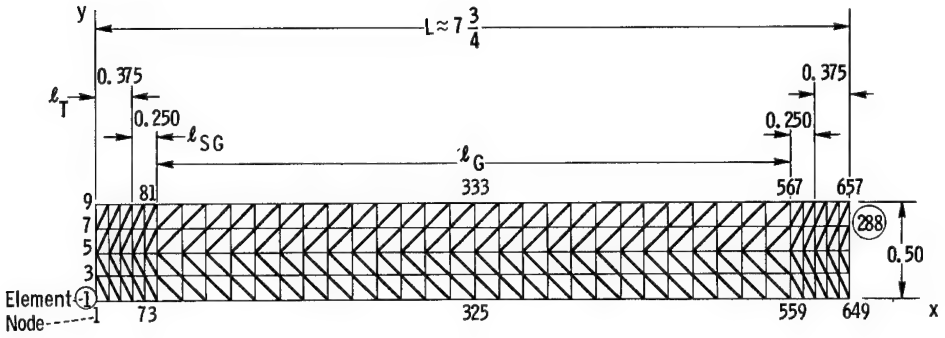

L Length of test section ℓ_G plus tapered portion of end tabs
ℓ_T Length of tapered portion of Micarta end tabs
ℓ_{SG} Section just beyond tapered portion of end tabs and site of top gages

Figure 1. - Grid for finite-element analysis of Mod I/E specimens. (Top gages located at nodes 74 and 77; midpoint gages located at nodes 326, 329, and 332. All dimensions shown are relative.)

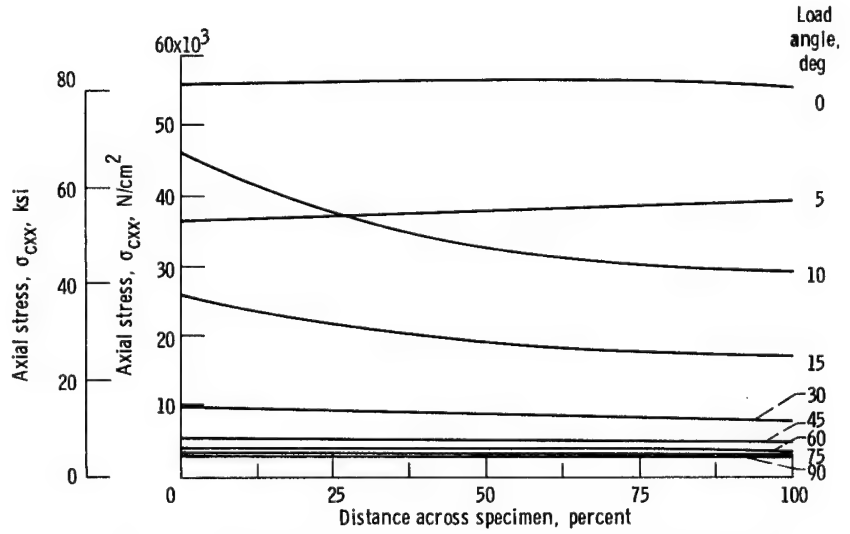

Figure 2. - Axial stress variation at tab ends for Mod I/E specimens for several load angles (finite-element analysis using the experimental fracture load for each specimen).

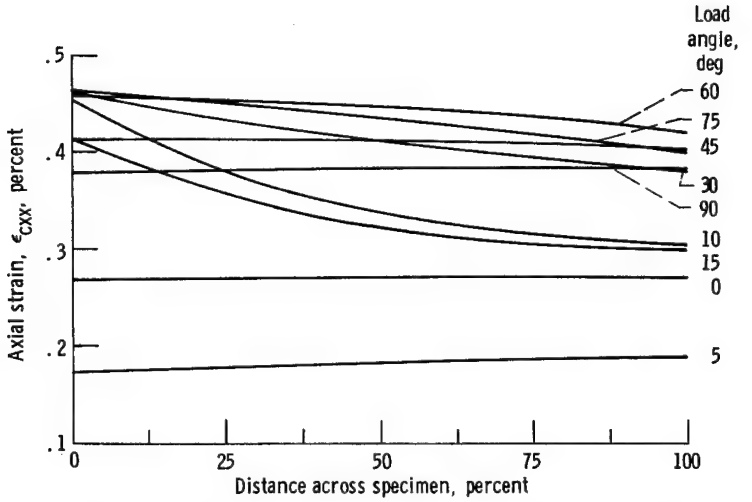

Figure 3. - Axial strain variation at tab ends for Mod I/E specimens for several load angles (finite-element analysis using the experimental fracture load for each specimen).

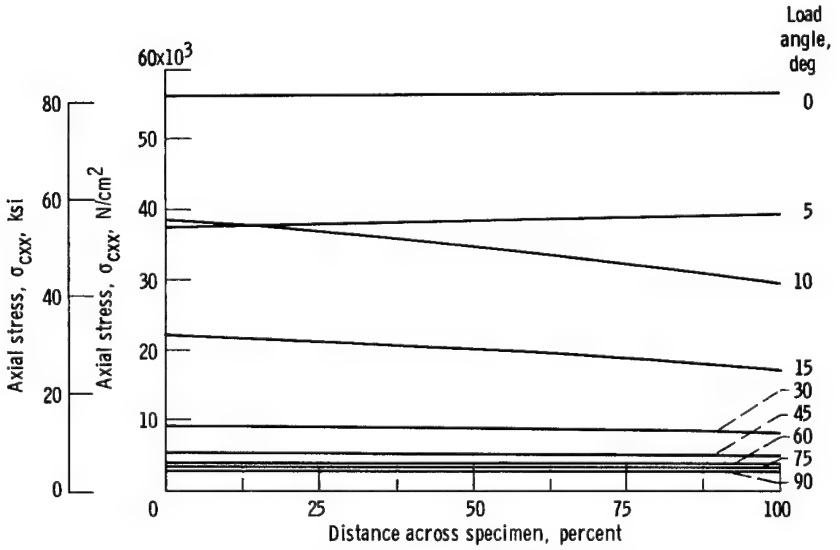

Figure 4. - Axial stress variation at midlengths for Mod I/E specimens for several load angles (finite-element analysis using the experimental fracture load for each specimen).

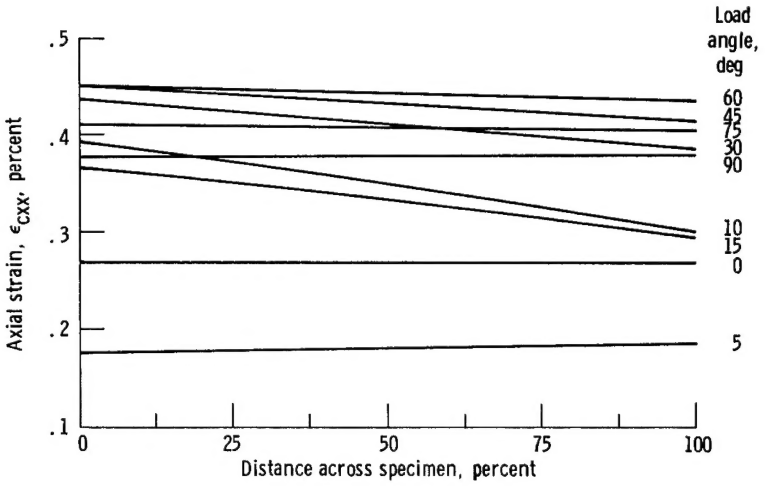

Figure 5. - Axial strain variation at midlengths for Mod I/E specimens for several load angles (finite-element analysis using the experimental fracture load for each specimen).

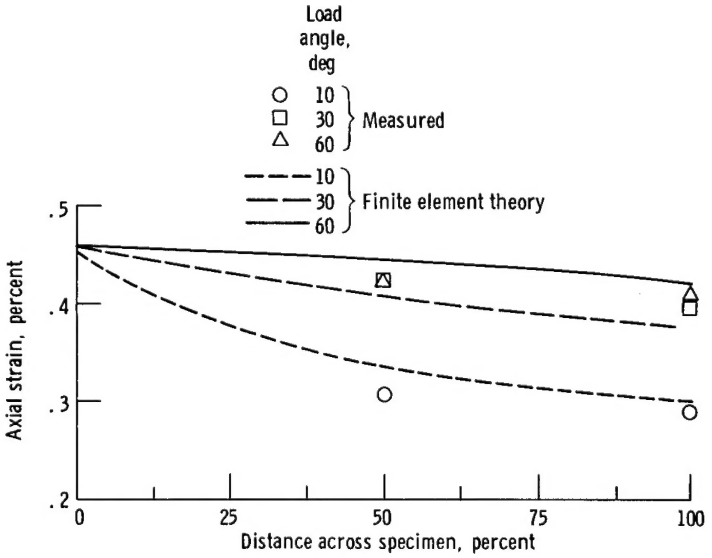

Figure 6. - Comparison at fracture load of predicted and measured axial strains near end tabs for off-axis specimens for Mod I/E.

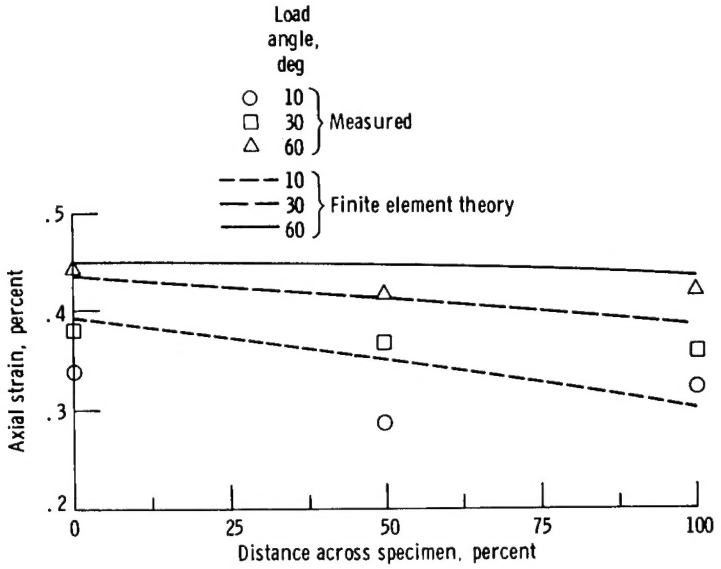

Figure 7. - Comparison at fracture load of predicted and measured axial strains at midlength of off-axis specimens from Mod I/E.

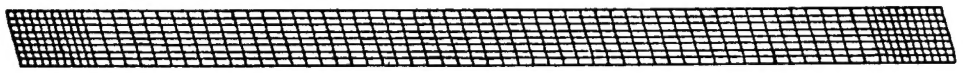

Figure 8. - NASTRAN model of off-axis specimen (657 nodes; 576 CQUAD2 elements).

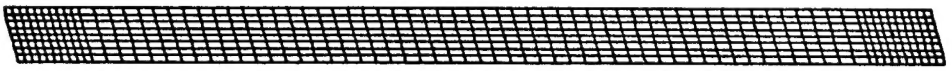

(a) Undeformed.

(b) Out-of-plane bending moment (11. 30 N· m (100 in· lb); maximum deflection, 4. 25 cm (1. 672 in.)).

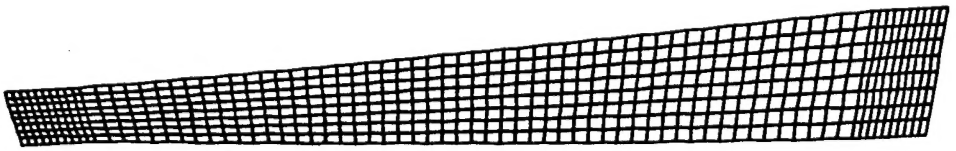

(c) Out-of-plane twisting moment (11. 30 N· m (100 in· lb); maximum deflection, 9. 29 cm (3. 658 in.)).

Figure 9. - NASTRAN plots of the 10^0 off-axis specimen showing deformed shapes due to out-of-plane eccentricities (Mod I/E).

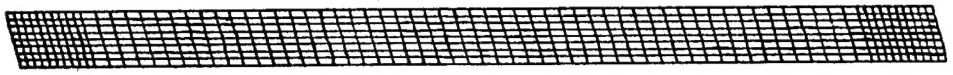

(a) Undeformed.

(b) Out-of-plane bending moment (11. 30 N · m (100 in · lb); maximum deflection, 16. 35 cm (6. 437 in.)).

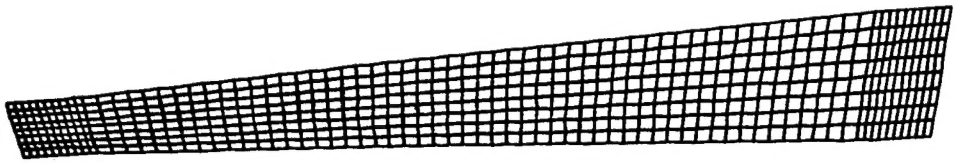

(c) Out-of-plane twisting moment (11. 30 N · m (100 in · lb); maximum deflection, 5. 72 cm (2. 250 in.)).

Figure 10. - NASTRAN plots of the 30° off-axis specimen showing deformed shapes due to out-of-plane eccentricities (Mod I/E).

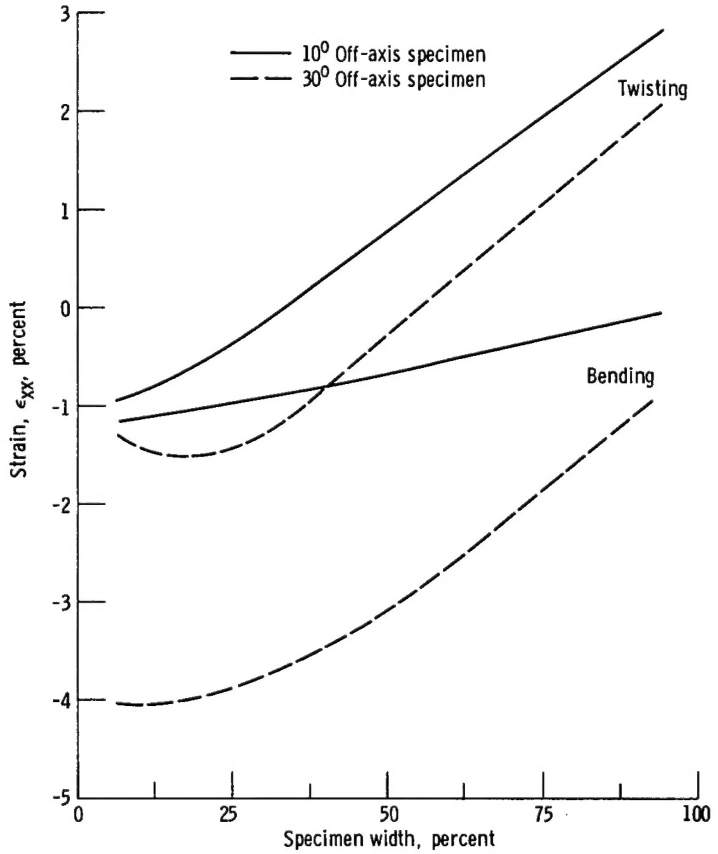

Figure 11. - Out-of-plane bending and twisting effects on axial strain near grips of 10° and 30° off-axis specimens from Mod I/E composites (11. 3 N · m (100 in · lb) moments).

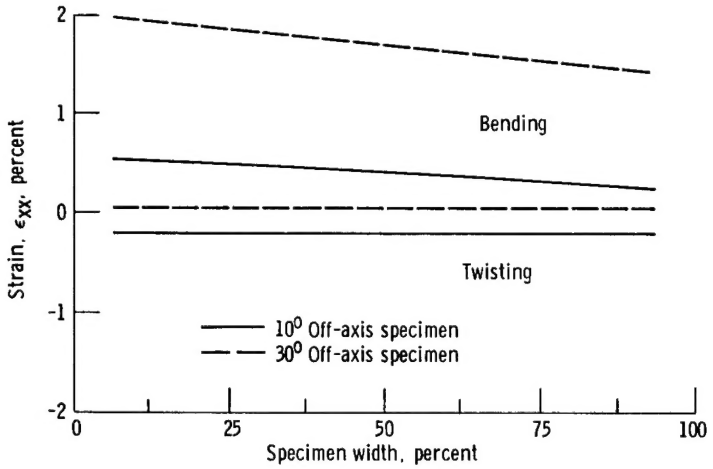

Figure 12. - Out-of-plane bending and twisting effects on axial strain at midlength of 10^0 and 30^0 off-axis specimens from Mod I/E composite (11.3-N·m (100-in·lb) moments).

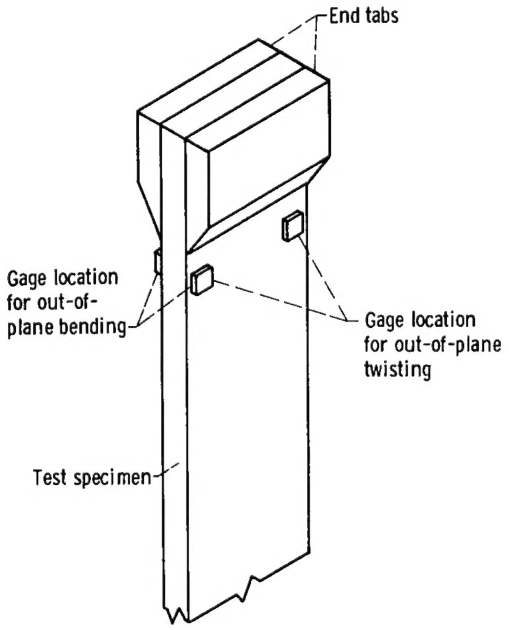

Figure 13. - Schematic depicting instrumentation to detect out-of-plane eccentricities during testing of off-axis fiber composites.

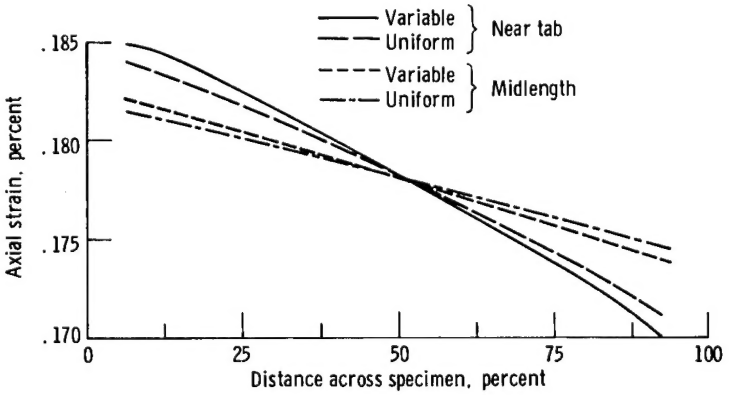

Figure 14. - Comparison of finite-element analysis results for 5^0 off-axis specimen (Mod I/E) showing effects of specimen thickness variation.